Hydrodynamic simulations of flow around a pile using turbulence-resolving models

A. Gilletta de Saint Joseph *FEM, Plouzané, France – alban.gilletta@france-energies-marines.org*
J. Chauchat *LEGI, Univ. Grenoble Alpes, Grenoble, France – julien.chauchat@univ-grenoble-alpes.fr*
C. Bonamy *LEGI, Univ. Grenoble Alpes, Grenoble, France – cyrille.bonamy@univ-grenoble-alpes.fr*
M. Robert *FEM, Plouzané, France – marie.robert@france-energies-marines.org*

ABSTRACT: With the increase of OWF in France, the question of sediment – flow – structure interactions has become essential. The interactions lead to the so-called scour process which is controlled by the flow vortices around the structure. To address this question, it is essential to have a reliable flow model. The aim of this contribution is to evaluate three turbulence modelling approaches: RANS, LES, hybrid RANS-LES and inlet boundary conditions to accurately predict the flow around the structure.

1 INTRODUCTION

With future objective of carbon neutrality by 2050, France is invested in the development of new renewable source of energy on its territory. As it is ranked second in terms of maritime space, the French bottom-fixed Offshore Wind Farms (OWF) the technical potential is estimated at 80 Giga Watts (GW), enough to provide about half of the national consumption. The English Channel is an important potential area benefiting from strong and steady wind over time and a moderate water depth to implement grounded structure. MOdelling of marine DUnes: Local and Large-scales EvolutionS in an OWF context (MODULLES) French project led by France Énergies Marines (FEM) focuses on the interactions between high and mobile submarine dunes and the future OWF off Dunkirk. This study is dedicated to small scale modelling of scour process around foundations of a single wind turbine facing turbulent current. The ability to predict how the scour process occurs around a wall-mounted circular cylinder is a major stake in order to size structures to protect them from damages. This phenomenon is driven by two hydrodynamical vortical structures namely the horseshoe vortex upstream the pile and the vortex-shedding downstream the pile. As these vortical structures are rather small, the required resolution for numerical simulation induces important computational cost. When the flow is highly turbulent, a way to capture the main eddies is to model turbulence. Different approaches exist, the most common model used in the engineering field is Reynolds Averaged Navier-Stokes (RANS). Advanced models, such as Large Eddy Simulations (LES) provide more accurate results by increasing the resolution part of turbulent structures while Hybrid RANS-LES models combine the two approaches. In this contribution, we analyze the accuracy of three turbulence modelling approaches, namely RANS, LES and hybrid RANS-LES to simulate the flow around a wall-mounted cylinder. An important technical question is the influence of the inlet boundary conditions especially for turbulence resolving

simulations (LES, hybrid RANS-LES). These two points are investigated using pimpleFOAM on two configurations: the plane channel flow and the wall-mounted cylinder case.

2 GOVERNING EQUATIONS

2.1 Navier-Stokes equations

When dealing with turbulence modelling, the Navier-Stokes equations are introducing the turbulent eddy viscosity, a fundamental parameter in turbulence modelling. Therefore these equations are presented by the coupled mass conservation equation (1) and momentum equation (2).

$$\frac{\partial \tilde{u}_i}{\partial x_i} = 0 \tag{1}$$

$$\frac{\partial \tilde{u}_i}{\partial t} + \frac{\partial}{\partial x_j}\left(\tilde{u}_i \tilde{u}_j\right) = \frac{-1}{\rho}\frac{\partial \tilde{p}}{\partial x_i} + \frac{\partial}{\partial x_j}\left[\left(\nu + \nu_t\right)\left(\frac{\partial \tilde{u}_i}{\partial x_j} + \frac{\partial \tilde{u}_j}{\partial x_i}\right)\right] \tag{2}$$

where u_i = velocity i^{th} component, p = modified pressure, ρ = fluid density, ν = kinematic viscosity, ν_t = turbulent eddy viscosity and ~ = time-averaging or filtering operator.

2.2 Turbulent eddy viscosity

RANS equations use time-averaging operator. The most widely used model is the k-ω SST model (Menter et al. 2003a) in which the turbulent eddy viscosity is defined as follows :

$$\nu_t = \frac{a_1 k}{max\left(a_1 \omega, S F_2\right)} \tag{3}$$

where a_1 = 0.31, k = Turbulent Kinetic Energy (TKE), ω = turbulent specific dissipation rate, S = invariant strain rate and F_2 = blending function.

Two transport equations for k and ω are added to close the system. This model behaves as a standard k-ω model in the viscous sublayer and as a k-ε model in the outer layer.

LES equations are obtained by applying a filtering operator to equations (1) and (2). In the Dynamic Lagrangian LES model (Meneveau et al. 1996), the turbulent eddy viscosity is defined in equation (4).

$$\nu_t = C(\boldsymbol{x}, t)\Delta^2|\bar{S}| \tag{4}$$

where C = function of **x** and t and Δ = integral scale of the subgrid-scale.

This model is part of the dynamic Smagorinsky group model in which C is no longer associated to classical Smagorinsky constant (Smagorinsky 1963) but varies over time and space. It enables more realistic turbulent features such as backscattering effect.

Hybrid RANS-LES combines both approaches. The switch between the two depends on the model used. This study focuses on the k-ω SST Scale Adaptative Simulation hybrid RANS-LES model (Menter & Egorov 2010b). By introducing a new term in the turbulent specific dissipation rate, based on a turbulent length scale defined as the velocity gradient over the velocity laplacian, the turbulent viscosity takes the value of the classical k-ω SST model when the flow is homogeneous and follows a classical Smagorinsky LES model when it is "disturbed".

2.3 Inlet boundary condition

One key issue to represent these vortical structures is to reproduce a well-developped turbulent flow at the inlet for turbulence-resolving model (Kirkil & Constantinescu 2015). While periodic boundary conditions are used as a reference for the plane channel flow configuration, two other approaches are tested for the wall-mounted cylinder: Divergence Free Synthetic Eddy Method (Poletto et al. 2013) and non-uniform boundary conditions implemented in OpenFOAM as turbulentDFSEM and GroovyBC respectively. DFSEM generates synthetic eddies based on random locations

and intensities while GroovyBC imposes a steady profile at the inlet. This study is mainly focusing on an influence of the inlet boundary conditions on the flow dynamic.

2.4 Configurations

Two configurations are studied in the present article. First, the plane channel flow configuration in order to assess best turbulent inlet boundary conditions. A first simulation using periodic boundary conditions succeeds in reproducing a converged fully developed turbulent flow, this simulation will be used as a reference. The computational domain is 20πH long, πH large and 1H high with H the water depth set to 0.06 m similarly to Fuhrman and co-workers experiment (Furman et al. 2010). The friction Reynolds number is often used to describe this configuration and is defined as follows:

$$Re_\tau = \frac{u_\tau H}{\nu} \quad (5)$$

Here $Re_\tau \approx 1000$. The wall-mounted cylinder configuration is similar to Roulund and co-workers experiment over a rigid bed (Roulund et al. 2005). The computational domain is 12D long, 8D wide and 1D high with D the cylinder diameter equal to 0.536 m. The friction Reynolds number is higher in this configuration, $Re_\tau \approx 7000$. Both configurations are shown in Figures 1-2.

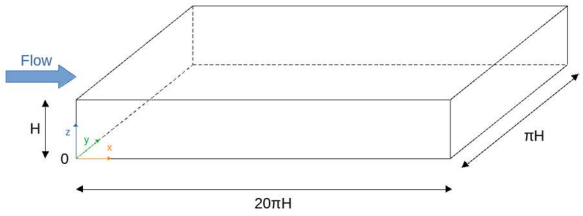

Figure 1. Plane channel configuration

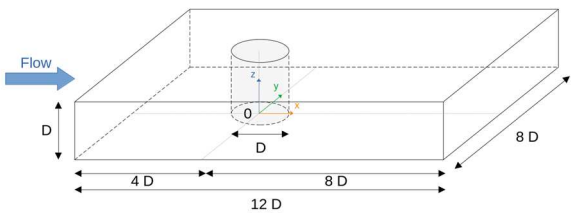

Figure 2. Wall-mounted cylinder configuration

3 RESULTS

This section is dedicated to simulations results of the two configurations performed with OpenFOAM.

3.1 Plane channel case

Figure 3 represents the streamwise profile of the friction velocity u_τ in the symmetry axis of the plane channel calculates as follows:

$$u_\tau = \sqrt{|\tau_{xy}|} \quad (6)$$

where τ_{xy} = bottom shear stress in the streamwise direction.

We introduce the notion of wall units defined as follows:

$$y^+ = \frac{y u_\tau}{\nu} \quad (7)$$

where y = distance to the wall or other length.

Three simulations are plotted using Dynamic Lagrangian LES model and same computational grid having a $z^+ = 6$, $y^+ = 30$ and $x^+ = 130$ respectively in the vertical, spanwise and streamwise directions in agreement with the resolution required for LES simulations (Métais 2018). The blue line corresponds to simulation using periodic boundary conditions and indicates an averaged friction velocity of 0.014 $m.s^{-1}$, slightly under the experimental value of 0.016 $m.s^{-1}$. Result from a RANS k-ω SST model using an imposed RANS profile boundary conditions with same mesh has

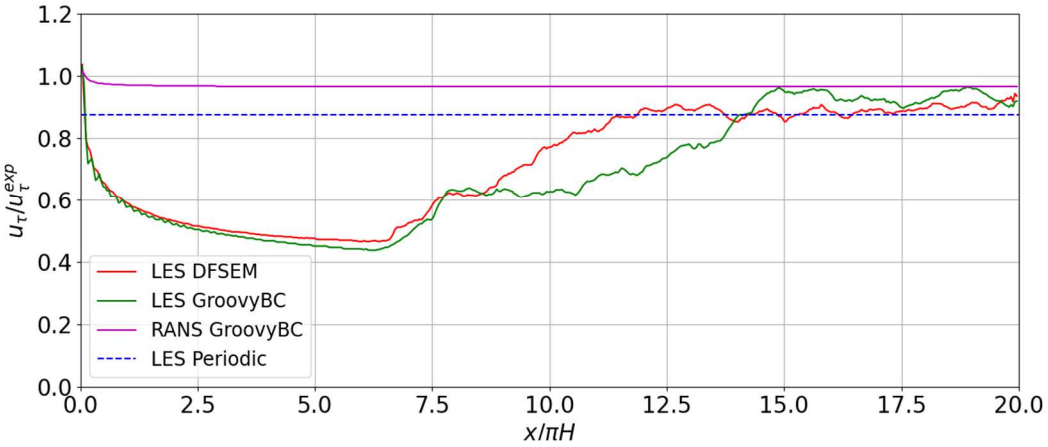

Figure 3. Time-averaged friction velocity profile in the symmetry axis

been added and shows a constant value close to the experimental friction velocity. LES simulations using imposed RANS profile and DFSEM inlet boundary conditions are quite similar since the friction value starts from the desired value due to the input parameter wished and drastically decays of about 50% until $x/\pi H \approx 6$. Then, they both increase until reaching the same value as the periodic boundary condition simulation. DFSEM reaches it sooner than the imposed RANS profile by about $2\pi H$.

Figure 4 represents three vertical profiles of the velocity, Reynolds stress and TKE scaled with experimental friction velocity. The average value for the periodic boundary condition simulation is taken over the entire computational domain while at least 25% of the channel length is taken for the three other simulations.

For all simulations, the velocity profiles are quite in fair agreement with the measurements represented by the blue crosses. Concerning the Reynolds stress, periodic boundary conditions has a linear expected shape likewise the RANS simulation but underestimates the maximum compared with the theory, that is to say $u_\tau^2 = 2.56 \times 10\text{-}4\ m^2.s^{-2}$. Without periodic boundary conditions, DFSEM results are

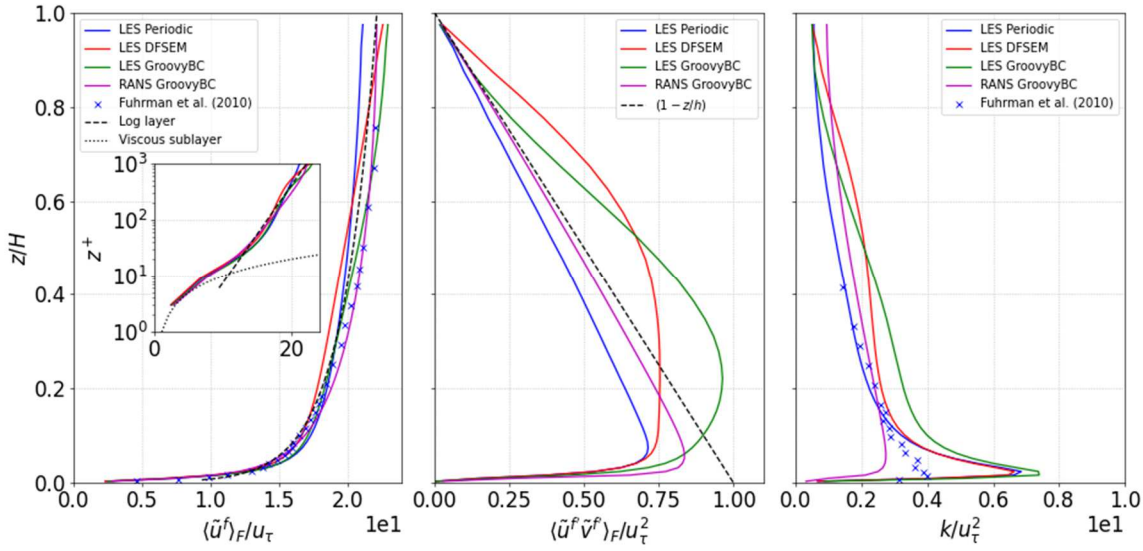

Figure 4. Time and space averaged velocity profile (left), Reynolds stress x-y component (centre) and TKE (right) with different inlet boundary conditions

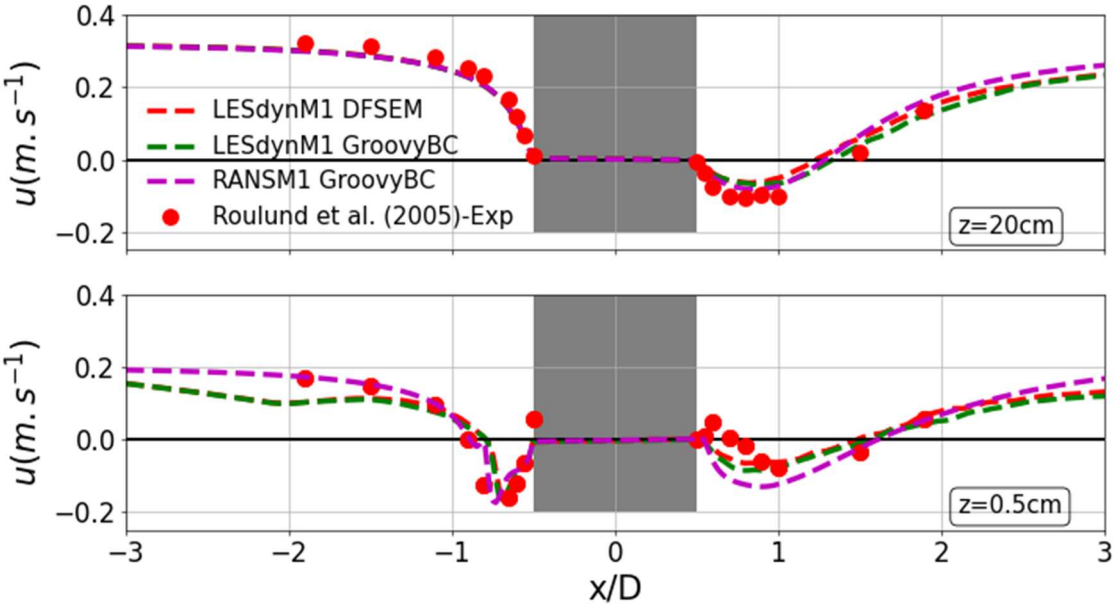

Figure 5. Time-averaged velocity profile of streamwise component in the symmetry plane at two elevations for Dynamic Lagrangian LES model.

quite good as the curve fits relatively well with the viscous sublayer profile but remains constant in the first part of the log layer and is overestimated. The linear expected profile is not retrieved with DFSEM, however it works better than imposed RANS profile where the Reynolds shear stress is overestimated in the log layer. Concerning the TKE vertical profile, the periodic boundary conditions simulation is in good agreement apart in the sublayer region where a peak is observed that is not present in the measurements and in RANS result. Complementary tests (not shown here) concluded that a finer mesh resolution reduces this peak. As the objective of this test is to evaluate inlet boundary condition, it clearly shows the superiority of DFSEM over the imposed RANS profile as the peak is intensified with the latter.

3.2 Wall-mounted cylinder case

3.2.1 Dynamic Lagrangian LES model

Figure 5 shows the streamwise velocity profile averaged in the symmetry axis in the vicinity of the cylinder over about 70 bulk time defined as follows :

$$T_b = \frac{H}{U} \tag{8}$$

Where U = 0.326 m.s^{-1} the average velocity.

The mesh used for all simulations is quite coarse with $z^+ = 4$, $y^+ = x^+ = 100$ for cells in the vicinity of the cylinder. The results are compared with Roulund and co-workers experiments (Roulund et al. 2005) and show overall good agreement. No important differences are observed between the two inlet boundary conditions. The main discrepancies are observed at the upstream and downstream side, on the near bed velocity that is underestimated. Whatever boundary conditions used, Dynamic Lagrangian LES model succeeds in representing the average streamwise velocity profile especially in the horseshoe vortex area where the velocity reaches a minimum value. The result from RANS k-ω SST, very similar, confirms the ability for LES model to reproduce mean velocity.

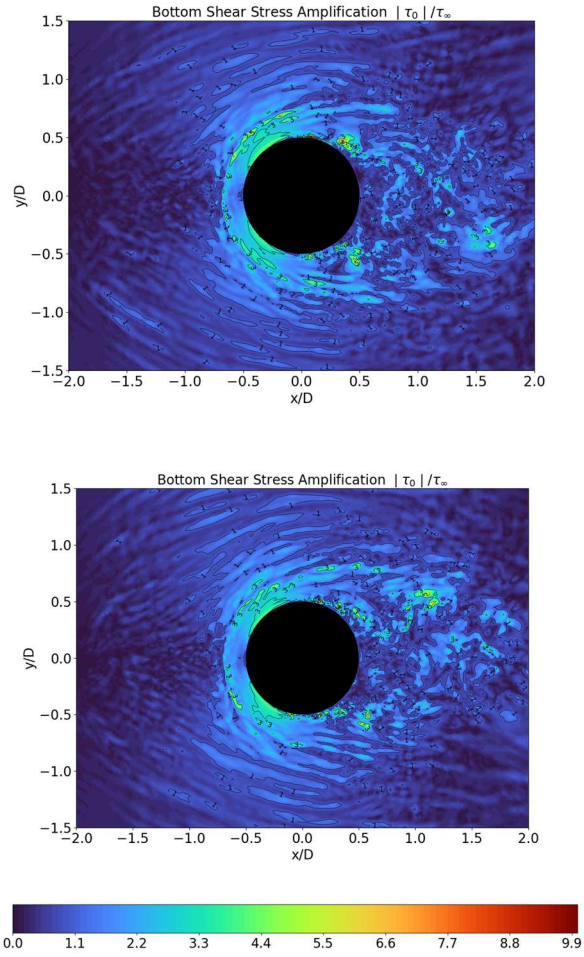

Figure 6. Averaged bed shear stress amplification with DFSEM boundary conditions (top) and GroovyBC boundary condition (bottom) for Dynamic Lagrangian LES model.

Figure 6 shows the time-averaged bed shear stress amplification map over 60 outputs for LES simulations using DFSEM boundary conditions in the top figure and imposed RANS profile in the bottom figure. The results are clearly not converged. When the average is taken over all time step, both simulations contain noises that represent extreme negative values far outside the expected range. This issue emphasizes the unstable behavior of Dynamic Lagrangian LES model for bed shear stress. Numerical schemes are probably the main reason of such instabilities. Therefore, Dynamic Lagrangian LES model fails in reproducing bed shear stress. As LES requires fine resolution and high computational cost, Hybrid RANS-LES models have been designed in order to reproduce more accurately the physical processes compared with RANS model, at an affordable cost. Results for k-ω SST-SAS Hybrid RANS-LES model are presented next.

3.2.2 k-ω SST-SAS Hybrid RANS-LES model

As mentioned previously, this model switches from RANS to LES mode if a perturbation of the flow is generated or detected such that the turbulent length scale defined is smaller than the length scale

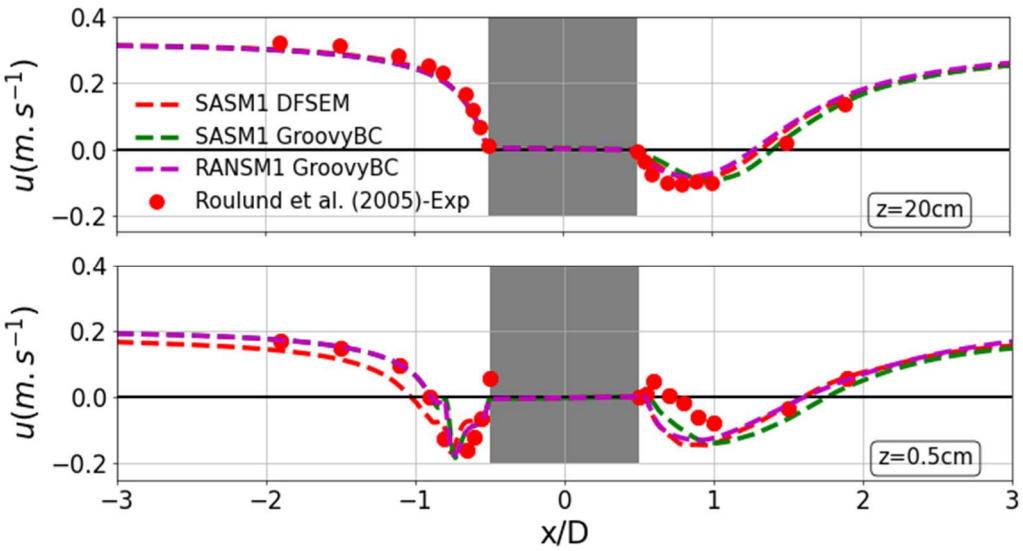

Figure 7. Time-averaged velocity profile of streamwise component in the symmetry plane at two elevations for k-ω SST-SAS Hybrid RANS-LES model.

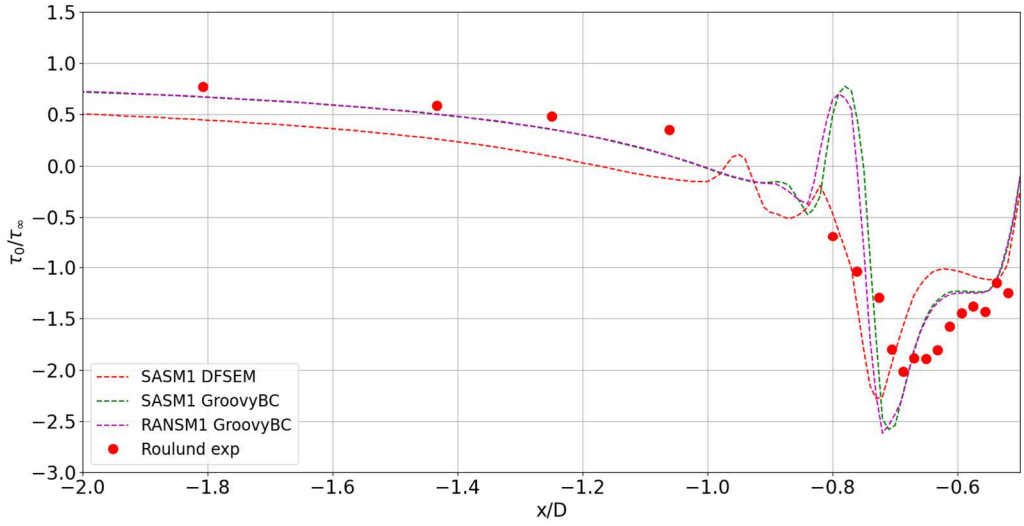

Figure 8. Time-averaged bottom shear stress amplification profile in the symmetry plane for k-ω SST-SAS Hybrid RANS-LES model.

modeled by the RANS model. In the plane channel case, there is no perturbation of the flow and the model behaves as a k-ω SST RANS model. In the wall-mounted cylinder case, the obstacle generates separated flow and disturbs the velocity so that the turbulence model is switched to the LES mode.

Figure 7 shows the velocity validation with the same mesh as the one used for the Dynamic Lagrangian LES model. Both boundary conditions give similar result except at the upstream side of the cylinder near the bed where DFSEM simulation slightly underestimates the velocity. Compared with LES simulations, the downstream near bed velocity is also underestimated by the Hybrid model. Despite this discrepancy, it can be infered that k-ω SST-SAS Hybrid RANS-LES model gives reasonable result. Adding to that, RANS result is closer to the imposed RANS profile hybrid simulation.

Figure 8 shows the time-averaged amplification of the bed shear stress profile upstream the obstacle over all time steps. Experimental results from Roulund and co-workers are shown as red dots. First, likewise Figure 7, RANS and hybrid simulations using imposed RANS profile give very similar result. It suggests that an imposed RANS profile boundary conditions prevents hybrid SAS model to switch from RANS to LES mode. Secondly, the two hybrid simulations give also similar results, which was not the case for LES results (not shown here). Both inlet boundary conditions reproduce the same patterns as the experiments with a minimum value representing the horseshoe vortex around -0.7D corresponding to an amplification of about 2. This minimum value is negative meaning that a reversing flow is taking place in this area, namely a clockwise rotating vortex. The main difference between the two simulations is the local maxima observed at -0.8D with imposed RANS profile simulation whereas two smaller ones are seen with DFSEM simulation at -0.8D and -0.9D.

The explanation of such a difference can be understood in Figure 9 representing snapshots of the simulations at two different times in the horseshoe vortex area. The results are colored by the spanwise vorticity. Experiments show that the horseshoe vortex

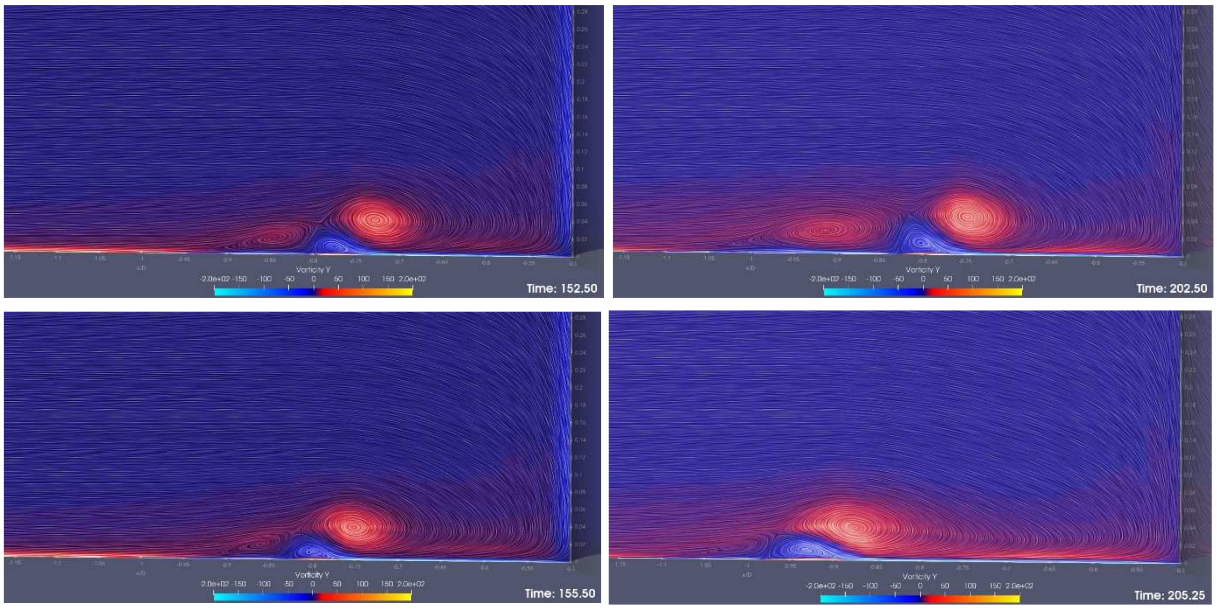

Figure 9. Instantaneous snapshots of spanwise vorticity with streamlines current for Groovy BC (left) and DFSEM (right) at the zero-flow mode (top) and the backflow mode (bottom).

is composed of several dynamic vortices (Baker 1980). In this figure, for both simulations, it is clearly observed, from downstream to upstream: one large primary clockwise vortex, one bottom-attached triangular counter clockwise vortex and one secondary clockwise vortex. Both simulations are able to reproduce vortex system. What is also seen from these snapshots is the dynamics of the system, evolving in a bimodal oscillation. The first mode takes place where all vortices move close to the cylinder, it is called the zero flow mode. The second mode takes place where all vortices move away from the cylinder and it is called the backflow mode (Kirkil & Constantinescu 2015). Snapshots from the two simulations represent these two modes. While the imposed RANS profile simulation shows a relatively short amplitude of about 0.02D between the two modes, DFSEM predicts a larger amplitude of 0.13D in better agreement with existing high Reynolds number simulations (Kirkil & Constantinescu 2015).

4 CONCLUSIONS

In this contribution, we demonstrate for the plane channel flow configuration that in order to establish a fully developed turbulent flow without periodic boundary conditions for LES simulations, either DFSEM or imposed RANS profile at the inlet boundary conditions can be used. However, the turbulence is establishing quite far away from the inlet, namely 13πH.

Implementing such a computational domain length in the LES simulations of wall-mounted cylinder case is difficult as it would increase drastically the computational cost. However because of the obstacle presence, no periodic boundary conditions can be used. No matter what inlet boundary conditions is used, both give unstable result in terms of wall shear stress using Dynamic Lagrangian LES model. k-ω SST−SAS Hybrid model gives almost as good result as LES model used in terms of velocity profile but is also much more stable for wall shear stress. With deeper analysis in the prediction of the horseshoe vortex, DFSEM can reproduce a more realistic vortices system than an imposed RANS profile that tends to prevent hybrid model to switch to LES mode and should be preferred.

5 ACKNOWLEDGEMENT

The authors gratefully acknowledge the support of the French project MODULLES partially funded by the ANR. We would like

to thank the Shom for its financial support and management. Most of the computations presented in this study were performed using LEGI laboratory cluster. We are thankful to the developers involved in OpenFOAM.

6 REFERENCES

Baker, C.J., 1980. The turbulent horseshoe vortex, Journal of Fluid Mechanics, 95, 347-367, doi:10.1017/S0022112079001506

Fuhrman, D.R., Dixen, M., Jacobsen, N.G., 2010. Physically-consistent wall boundary conditions for the k-ω turbulence model. Journal oh Hydraulic Researh, 48, 793-800, doi:10.1080/00221686.531100

Kirkil, G., Constantinescu, G., 2015. Effects of cylinder Reynolds number on the turbulent horseshoe vortex system and near wake of a surface-mounted circular cylinder. Physics of Fluids, 27, 075-102, doi:10.1063/1.4923063

Meneveau, C., Lund, T., Cabot, W., 1996. A Lagrangian dynamic subgrid-scale model of turbulence. Journal of Fluid Mechanics, 319, 353-385, doi:10.1017/S0022112096007379

Menter, F.R., Kuntz, M., Langtry, R., 2003a. Ten years of industrial experience with the SST turbulence model. Proceedings of the fourth international symposium on turbulence, heat and mass transfer, 625-632

Menter, F.R., Egorov, Y., 2010b. A scale-adaptative simulation method for unsteady turbulent flow predictions - Part 1: Theory and model description. Flow Turbulence Combust, 85, 113-138, doi:10.1007/s10494-010-9264-5

Métais, O., 2018. Large Eddy Simulation of Turbulence : Fundamentals and Applications – Lectures notes. Grenoble

Poletto, R., Craft, T., Revell, A., 2013. A New Divergence Free Synthetic Eddy Method of the Reproduction of Inlet Flow Condition for LES. Flow Turbulence and Combustion, 91, 519-539, doi:10.1007/s10494-013-9488-2

Roulund, A., Sumer, B.M., Fredøe, J., Michelsen, J., 2005. Numerical and experimental investigation of flow and scour around a circular pile. Journal of Fluid Mechanics, 534, 351-401, doi:10.1017/S0022112005004507

Smagorinsky, J., 1963. General circulation experiments with the primitive equations. Monthly Weather Review, 91, 99-164, doi:10.1175/1520-0493(1963)091<0099:GCEWTP>2.3CO;2

Soulsby, R.L., 1983. The Bottom Boundary Layer of Shelf Seas, in Elsevier Oceanography Series. Elsevier, 189-266

Dissertation

Roden, J.E., 1998. The sedimentology and dynamics of mega-dunes, Jamuna River, Bangladesh. PhD Thesis. University of Leeds, UK, 310pp